

Controlling coupled magnons with pumps

Fan Yang(杨帆), Chenxiao Wang(王辰笑), Zhijian Chen(陈志坚), Kaixin Zhao(赵恺欣), Weihao Liu(刘炜豪), Shuhuan Ma(马舒寰), Chunke Wei(魏纯可), Jiantao Song(宋剑涛), Jinwei Rao(饶金威), and Bimu Yao(姚碧霖)
Citation: Chin. Phys. B, 2025, 34 (**10**): 107508. DOI: 10.1088/1674-1056/addce3
http://cpb.iphy.ac.cn; http://iopscience.iop.org/cpb

What follows is a list of articles you may be interested in

Effect of interlayer interaction on magnon properties of vdW honeycomb heterostructures

Jun Shan(单俊), Lichuan Zhang(张礼川), Huasu Fu(付华宿), Yuee Xie(谢月娥), Yuriy Mokrousov, and Yuanping Chen(陈元平)
Chin. Phys. B, 2025, 34 (**8**): 087501. DOI: 10.1088/1674-1056/adce97

Bifurcation of the bound states in the continuum in a dissipative cavity magnonic system

Xinlin Mi(米锌林), Lijun Yan(闫丽君), Bimu Yao(姚碧霖), Shishen Yan(颜世申), Jinwei Rao(饶金威), and Lihui Bai(柏利慧)
Chin. Phys. B, 2025, 34 (**6**): 067508. DOI: 10.1088/1674-1056/add4e4

Magnon behavior in YIG film under microwave excitation investigated by Brillouin light scattering

Guofu Xu(徐国服), Kang An(安康), Wenjun Ma(马文俊), Xiling Li(李喜玲), C. K. Ong, Chi Zhang(张驰), and Guozhi Chai(柴国志)
Chin. Phys. B, 2025, 34 (**6**): 067507. DOI: 10.1088/1674-1056/add24c

Strain-manipulated dispersion characteristics of magnonic crystals with Dzyaloshinskii-Moriya interaction and applications on spin-wave devices

Chuhan Zhou(周楚涵), Xiaotian Jiao(焦晓天), Jiaxi Xu(徐佳熙), Zhaonian Jin(金兆年), Lin Chen(陈琳), and Zhikuo Tao(陶志阔)
Chin. Phys. B, 2025, 34 (**2**): 027501. DOI: 10.1088/1674-1056/ad9892

Alternating spin splitting of electronic and magnon bands in two-dimensional altermagnetic materials

Qian Wang(王乾), Da-Wei Wu(邬大为), Guang-Hua Guo(郭光华), Meng-Qiu Long(龙孟秋), and Yun-Peng Wang(王云鹏)
Chin. Phys. B, 2024, 33 (**9**): 097507. DOI: 10.1088/1674-1056/ad6425

TOPICAL REVIEW — Advanced magnonics

Controlling coupled magnons with pumps

Fan Yang(杨帆)[1,†], Chenxiao Wang(王辰笑)[1,†], Zhijian Chen(陈志坚)[1], Kaixin Zhao(赵恺欣)[1], Weihao Liu(刘炜豪)[2], Shuhuan Ma(马舒寰)[1], Chunke Wei(魏纯可)[2], Jiantao Song(宋剑涛)[1], Jinwei Rao(饶金威)[3,‡], and Bimu Yao(姚碧霖)[1,2,§]

[1] *School of Physical Science and Technology, ShanghaiTech University, Shanghai* 201210, *China*
[2] *State Key Laboratory of Infrared Physics, Shanghai Institute of Technical Physics, Chinese Academy of Sciences, Shanghai* 200083, *China*
[3] *School of Physics, Shandong University, Jinan* 250100, *China*

(Received 31 March 2025; revised manuscript received 20 May 2025; accepted manuscript online 27 May 2025)

Strong coupling effects in magnonic systems are highly promising. They combine the advantages of different quasiparticles and enable energy transfer for coherent information processing. When driven by microwave, electric, or optical pumps, these coupling effects can give rise to intriguing nonlinear phenomena, which have become a focal point in the field of magnonics. This review systematically explores pump-engineered magnon-coupling systems from three perspectives: (1) pump-induced hybridization of magnon modes, (2) nonlinear manipulation of magnon dynamics, and (3) implementation of functional magnonic devices. Unlike conventional cavity–magnon interactions that are constrained by electromagnetic boundaries, pumped coupled magnons are liberated from these restrictions. They can operate over a broad frequency band rather than being confined to discrete modes. An example is the recently discovered pump-induced magnon mode (PIM). These magnons arise from the collective excitations of unsaturated spins driven by microwave pumps. They exhibit reduced damping and photon-number-sensitive splitting characteristics, facilitating waveform-controlled coupling strength and enhanced nonlinearity — features that support phenomena such as magnonic frequency combs (MFCs). By expanding this principle to electric pumping schemes, we bridge fundamental physics and practical device applications, enabling nonreciprocal switching and meter-scale strong coupling. These advances establish high-dimensional control capabilities for coupled magnonics and pave the way for their use as a promising platform for dynamically programmable devices, magnetic-field sensing, and coherent networks.

Keywords: magnon, strong coupling, magnonic frequency comb, spintronics

PACS: 76.50.+g, 75.30.Ds, 85.70.Ge, 85.75.–d

DOI: 10.1088/1674-1056/addce3 **CSTR:** 32038.14.CPB.addce3

1. Introduction

Light–matter interaction, which serves as a cornerstone of photodetection, occupies a key position in advanced information processing. Its critical role becomes particularly evident in weak-signal detection regimes — from single-photon counting[1,2] and deep-space communication[3–5] to biofluorescence tracking[6,7] — where detection efficiency fundamentally governs the system's signal-to-noise ratio and, consequently, its sensitivity. This capability has enabled a wide range of applications across civilian, military, and commercial domains. Recent advances in strong-coupling physics have revolutionized photoelectric conversion, including enhanced electronic transport via hybridized states in quantum devices,[8] cavity-enhanced charge conductivity,[9] and current enhancement in strongly coupled organic semiconductors and plasmonic modes.[10] Novel properties have also been discovered in nonequilibrium coupled systems, demonstrating coupling enhancement through photocarriers,[11] ultrafast lasers,[12] local strain,[13] and dynamical condensates controlled by voltage.[14] These dynamic control mechanisms have transcended the limitations of conventional equilibrium systems, bridging fundamental physics and functional device engineering.

Platforms for studying strong light–matter coupling include cavity quantum electrodynamics (QED) systems with excitons,[15] phonons,[16] and plasmons.[17] These systems enable the precise measurement and manipulation of individual quantum systems, advancing the realization of quantum computers. For his groundbreaking contributions to cavity-QED, Serge Haroche was awarded the 2012 Nobel Prize. Magnons, as collective spin excitations, are rapidly gaining attention due to their potential as a complementary technology to CMOS and their applicability in wave-based computing and devices. Magnonic systems offer several unique advantages: their high spin density ($\sim 10^{22}$ cm^{-3})[18,19] enhances their interaction strength with photons, their low Gilbert damping coefficient (down to 10^{-5} in yttrium iron garnet, YIG)[20] ensures long coherence times, and their charge neutrality and

†These authors contributed equally to this work.
‡Corresponding author. E-mail: raojw@sdu.edu.cn
§Corresponding author. E-mail: yaobimu@mail.sitp.ac.cn

© 2025 Chinese Physical Society and IOP Publishing Ltd. All rights, including for text and data mining, AI training, and similar technologies, are reserved.

millimeter-scale spin wave propagation[21] help to minimize ohmic losses. Moreover, magnons possess excellent tunability and can readily couple directly or indirectly with microwave photons, optical photons, phonons, and quantum circuits. This enables the integration of complementary physical properties and facilitates coherent information transfer across diverse material platforms.

The utilization of strongly coupled magnon systems and the control of their coupling strength (or Rabi oscillations) are key to advancing magnon-based technologies. However, dynamically controlling these strongly coupled magnonic systems remains challenging, as the photon–magnon coupling strength is typically fixed once the system is configured.[22] It is often modified only through inefficient "static" approaches, such as cavity redesign, material optimization, or resetting the mode overlap. These limitations hinder the real-time modulation of polariton states and constrain the development of programmable magnonic devices and reconfigurable logic gates. Overcoming these constraints is essential for the realization of functional magnonic technologies.

In this article, we review how pumping creates new ways to control strong coupling in magnonic systems. Pumps introduce additional degrees of freedom from external fields beyond the intrinsic coupled system. By simply varying the parameters of the pump, such as electromagnetic waves or bias voltage, the coupling strength can be freely tuned without the need to reconfigure the subsystems. This decouples the tuning process from constraints imposed by the electromagnetic boundaries of cavities or material structures. In terms of coupled-state construction, pumping enables the connection of magnons with other quasiparticles, allowing for on-demand enhancement or suppression of coupling strength (up to the ultrastrong regime). The resulting hybrid states form the basis for multidimensional tunability of coupling. Regarding control performance, precise and continuous modulation of the coupled states can be achieved through adjustments to the pump's power, frequency, phase, and polarization. Pumping can also drive the coupled magnonic system into nonlinear regimes, giving rise to phenomena such as multistability, chaos, and frequency mixing. These effects underpin the recent development of magnonic frequency combs (MFCs). From the perspective of device functionality, the flexibility of pump control expands operational capabilities, offering advantages for signal transmission, amplification, radiation, logic operations, and data storage. Leveraging the advanced tunability afforded by pump control opens promising pathways for the dynamic manipulation of coupled magnon states.

2. Pumped magnon dynamics

Magnons, the quasiparticles associated with collective spin excitations in magnetic materials, have attracted considerable attention as information carriers in hybrid systems.[23] In magnetic insulators, magnons propagate without the involvement of conduction electrons,[24] thereby eliminating ohmic losses. Moreover, due to the intrinsic isolation of spin degrees of freedom from environmental noise, magnons exhibit a low loss rate (on the order of megahertz[25]) and possess a long coherence length reaching several tens of micrometers or even up to millimeters.[26,27]

Apart from these favorable transport properties, magnons can coherently interact with a wide range of quantum and classical systems, such as superconducting qubits,[28–30] phonons,[31,32] microwave photons,[33,34] and optical photons,[35,36] through mechanisms including virtual photon exchange, magnetostrictive interaction, dipolar interactions, and exchange coupling. Strong light–matter coupling allows two distant systems to exchange information under external control. In the microwave regime, cavity magnon polaritons (CMPs) are hybrid quasiparticles that emerge from the strong coherent coupling between collective spin excitations (magnons) in a magnetic material and the electromagnetic field (photons) confined in a microwave cavity. This coupling is mediated by the magnetic dipole interaction and gives rise to new hybridized eigenmodes. CMPs,[37] which combine the high-speed nature of photons with the low-loss, long-lifetime features of magnons, offer a route to spin-based cavity QED and high-performance hybrid spintronic devices.

Beyond establishing coupling between magnons and cavity photons, preserving coherence during information transduction requires the coupling strength g to exceed the dissipation rates κ_1 and κ_2 of the respective subsystems. This requirement is quantified by $g/\kappa_1 > 1$, $g/\kappa_2 > 1$, defining the strong coupling regime essential for coherent information operations.[38] Strong coupling between magnons and cavity photons began with Soykal and Flatté's 2010 theory of quantum-coherent magnon–photon interaction in a ferromagnetic nanomagnet[39] and the first experimental realization of hybridization at low temperatures by Huebl *et al.* in 2013.[25] While the preceding discussion focuses on coherent coupling, characterized by level repulsion in the dispersion and linewidth attraction, the practical implementation of integrated devices necessitates the consideration of open systems. In open systems, dissipative coupling naturally arises.[40–42] It exhibits the exact opposite behavior — level attraction in the dispersion and linewidth repulsion.[43] Dissipative coupling offers a way to realize nonreciprocal signal transmission[42,44] and also contributes to chiral magnonics through unidirectional coupling and energy accumulation.[45–47]

In a given magnonic system, direct control over magnon–photon coupling remains limited. Conventional tuning methods, such as modifying the cavity structure or adjusting the magnetic sample's position, are inherently slow, often exceeding the signal lifetime. Consequently, real-time modulation of coupling becomes difficult. Pump-based control offers a po-

tential solution, as it enables *in situ* tuning of magnon–photon coupling.[22]

A pump can drive magnons across a broad range of frequencies, each relying on distinct physical mechanisms. Acoustic waves, either surface or bulk, excite spin waves via magnetoelastic coupling in ferro- and antiferromagnetic materials,[51,58] offering the advantage of low-loss operation. Optical pumping induces magnon dynamics through magneto–optical interactions[53,59] and is particularly suited for ultrafast information processing.[60] Owing to their gigahertz-range eigenfrequencies, magnons directly couple to microwave photons via magnetic dipole interactions, making microwave pumping a particularly direct and efficient method for magnon control.[22,38,43,61]

So far, various microwave pumping techniques have been developed, including continuous-wave (CW) pumping,[49] short-pulsed pump–probe methods,[48,62] incoherent (noise) pumping,[50] and Floquet engineering (temporal modulation by periodic drives),[22,63] etc. By modulating the power,[22,29,52,57] frequency,[22,52,57] and phase of microwave pumps,[64,65] we can flexibly control the temporal evolution of magnon states, as well as their interactions with other excitations.

When magnon systems absorb sufficient pump energy to exceed critical thresholds, their dynamics exhibit a range of intriguing nonlinear behaviors.[52,54,55] For instance, direct microwave pumping can induce Bose–Einstein condensation (BEC) of magnons at room temperature,[66,67] where a macroscopic population of magnons accumulates at the lowest energy state. In addition to individual magnon dynamics, richer nonlinear phenomena emerge in coupled systems. In cavity magnonic systems, the strong coupling between magnons and cavity photons leads to bistability of CMPs under microwave pumping.[52] Furthermore, in coupled magnon systems, MFCs can be generated through four-magnon scattering or the magnetostrictive effect.[55,68]

These nonlinear phenomena provide an important physical basis for the development of functional magnonic devices. For instance, the BEC of pumped magnons has enabled magnon lasers, which serve as coherent magnon sources for magnonic circuits.[54] The bistability of CMPs facilitates the development of switching devices with controllable state transitions.[52] Extending this further, multistability offers multivalued logic capabilities without increasing system complexity or requiring additional components.[69] Additionally, MFCs[68,70] have practical applications in frequency conversion[52] and measurement,[68,70] significantly advancing the development of nonlinear magnonic devices, as shown in Fig. 1.

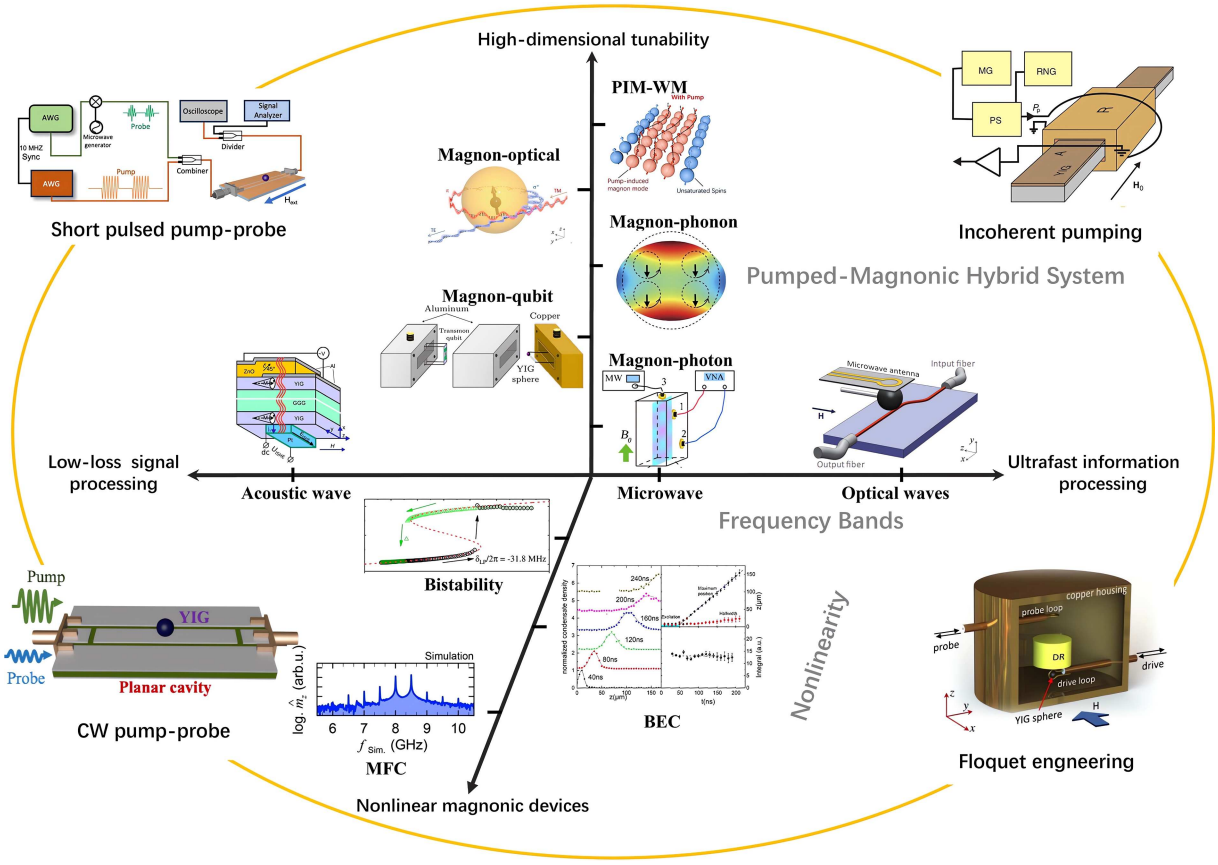


Fig. 1. Overview of pump-driven magnonic hybrid systems and their functionalities. Frequency bands ranging from acoustic and microwave to optical frequencies enable coherent and nonlinear control of magnon interactions across different platforms. These interactions underpin diverse nonlinear phenomena, including bistability, BEC, and MFCs, offering pathways toward tunable, reconfigurable, and low-loss magnonic devices for coherent signal processing and hybrid quantum systems. Reproduced with permission from Refs. [22,29,48–57].

3. Pump-induced continuous coupled magnon states

Recent experimental advances have demonstrated a series of continuous pump-induced coupled magnon states, in which the parameters of the magnonic systems are dynamically controlled via different forms of pump. As summarized in Figs. 2(a)–2(f), various physical mechanisms have been employed to engineer coherent, nonlinear, and hybridized magnon states that evolve smoothly with the pump parameters such as frequency and power.

3.1. Continuously tunable qubit–magnon splitting via double dressing

In Fig. 2(a), a qubit–magnon hybrid system is subject to an external microwave drive applied directly to the qubit.[29] The system is governed by a time-dependent Hamiltonian

$$\hat{H}/\hbar = \frac{1}{2}\omega_{\rm q}\sigma_z + \omega_{\rm m}\hat{b}^\dagger\hat{b} + g_{\rm qm}(\sigma_+\hat{b} + \sigma_-\hat{b}^\dagger) + \frac{1}{4}\Omega_{\rm d}(\sigma_+ {\rm e}^{-{\rm i}\omega_{\rm d}t} + \sigma_- {\rm e}^{{\rm i}\omega_{\rm d}t}). \quad (1)$$

Here, $\omega_{\rm q}$ and $\omega_{\rm m}$ are the frequencies of the qubit and magnon modes, associated with the Pauli operators σ_z, $\sigma_\pm$ and the magnon annihilation operator $\hat{b}$, respectively; $g_{\rm qm}$ represents the strength of the qubit–magnon coupling, while $\Omega_{\rm d}$ and $\omega_{\rm d}$ denote the strength and frequency of the external microwave pump.

At zero detuning ($\omega_{\rm q} = \omega_{\rm m}$), the system exhibits four resonant peaks due to the emergence of doubly dressed states. The outer and inner frequency splittings evolve continuously with increasing drive power, revealing symmetric particle–hole behavior. As shown in Fig. 2(a) (right), the theoretical prediction based on the driven Hamiltonian matches the experimental data with excellent accuracy, confirming the controlled tunability and underlying hybridization dynamics.

3.2. Suppression of magnon–photon coupling via Suhl instability

A representative example of the pump-induced effect in magnon–photon coupled systems is the suppression of the magnon–photon coupling based on the Suhl instability. The onset of Suhl instability in cavity magnonics can be described by an effective Hamiltonian

$$\hat{\mathcal{H}} = \hat{\mathcal{H}}_1 + \hat{\mathcal{H}}_2 + \hat{\mathcal{H}}_3. \quad (2)$$

The microwave drive term is

$$\hat{\mathcal{H}}_1/\hbar = \left[h{\rm e}^{-{\rm i}\omega t}\left(U_{\rm r}\hat{b}^\dagger + U_0\hat{b}_0^\dagger\right) + {\rm H.c.}\right], \quad (3)$$

and the linear interaction reads

$$\hat{\mathcal{H}}_2/\hbar = \omega_{\rm c}\hat{b}^\dagger\hat{b} + \omega_0\hat{b}_0^\dagger\hat{b}_0 + \left[g_0\hat{b}_0^\dagger\hat{b} + {\rm H.c.}\right] + \sum_{k\neq 0}\omega_k\hat{b}_k^\dagger\hat{b}_k. \quad (4)$$

Here, $\omega_{\rm c}$ and $\hat{b}_0$ denote the annihilation operators for the cavity and Kittel modes, respectively; their frequency is ω_0, and g_0 is their coupling strength. The pump field with amplitude h and frequency ω couples to both modes via $U_{\rm r}$ and U_0. The nonlinear three-magnon process is represented by

$$\hat{\mathcal{H}}_3/\hbar = \frac{1}{2}\sum_{k\neq 0}\left(V_k\hat{b}_0\hat{b}_k^\dagger\hat{b}_{-k}^\dagger + {\rm H.c.}\right). \quad (5)$$

It describes the decay of a Kittel magnon into a pair of spin waves via three-magnon scattering, with nonlinear coupling V_k.

As illustrated in Fig. 2(b), increasing pump power activates a nonlinear three-magnon scattering channel, which redistributes energy from the Kittel mode into high-k spin-wave excitations. This back-reaction progressively suppresses the magnon–photon coupling, leading to the reduction and eventual collapse of the avoided crossing. The magnitude of the magnon–photon splitting thus becomes continuously tunable via the pump power. When nonlinear damping dominates, the avoided crossing collapses entirely. This illustrates how the spin-wave back-reaction reshapes the spectral structure according to the pump power[71] offering a new route for dynamic control of CMP behavior through pumping.

3.3. Floquet-modulated magnon–photon hybrid splitting via Autler–Townes splitting and floquet ultrastrong coupling

Floquet engineering refers to the control of quantum systems through time-periodic modulation of system parameters.[72,73] In analogy with Bloch's theorem in spatially periodic systems, the Floquet theorem allows time-periodic Hamiltonians to yield a spectrum of quasi-energy states, known as Floquet states. These states provide an intuitive framework with which to understand the stroboscopic dynamics of driven systems. Originally developed in atomic and condensed matter systems, Floquet techniques are now widely used to engineer hybrid interactions and induce novel nonequilibrium phenomena, such as coherent control of coupling strength.[22]

The Floquet modulation of the magnon–photon coupling is realized by applying an alternative drive to periodically modulate the magnon frequency. This Floquet cavity magnonic system can be described by a time-periodic Hamiltonian

$$\hat{H}/\hbar = \omega_{\rm c}\hat{c}^\dagger\hat{c} + \omega_{\rm m}\hat{b}^\dagger\hat{b} + J(\hat{c}^\dagger\hat{b} + \hat{c}\hat{b}^\dagger) + \Omega\hat{b}^\dagger\hat{b}\cos(\omega_{\rm D}t), \quad (6)$$

where J is the coherent magnon–photon coupling strength, and the last term represents a Floquet drive applied to the magnon mode, with amplitude Ω and frequency $\omega_{\rm D}$.

As shown in the right panel of Fig. 2(c), this configuration provides two independent tuning parameters — the amplitude and frequency of the drive field — enabling precise *in-situ* modulation of the magnon–photon coupling strength. It reveals a drive-controlled tunable hybridization and leads

to magnonic Autler–Townes splitting (ATS), where the mode separation varies continuously with the drive strength. ATS, originally observed in atomic physics,[74] describes the splitting of energy levels into doublets under the influence of a strong coherent field, where the splitting magnitude directly proportional to the drive strength and there is no reliance on quantum interference.[75] As the drive strength increases, the Floquet-induced mode splitting can approach or exceed the energy level spacing between the two interacting modes, marking the onset of the Floquet ultrastrong coupling (FUSC) regime. Unlike conventional ultrastrong coupling, FUSC is characterized by both the breakdown of the rotating-wave approximation and a dynamically induced splitting that surpasses the level separation, representing a fundamentally distinct mechanism.

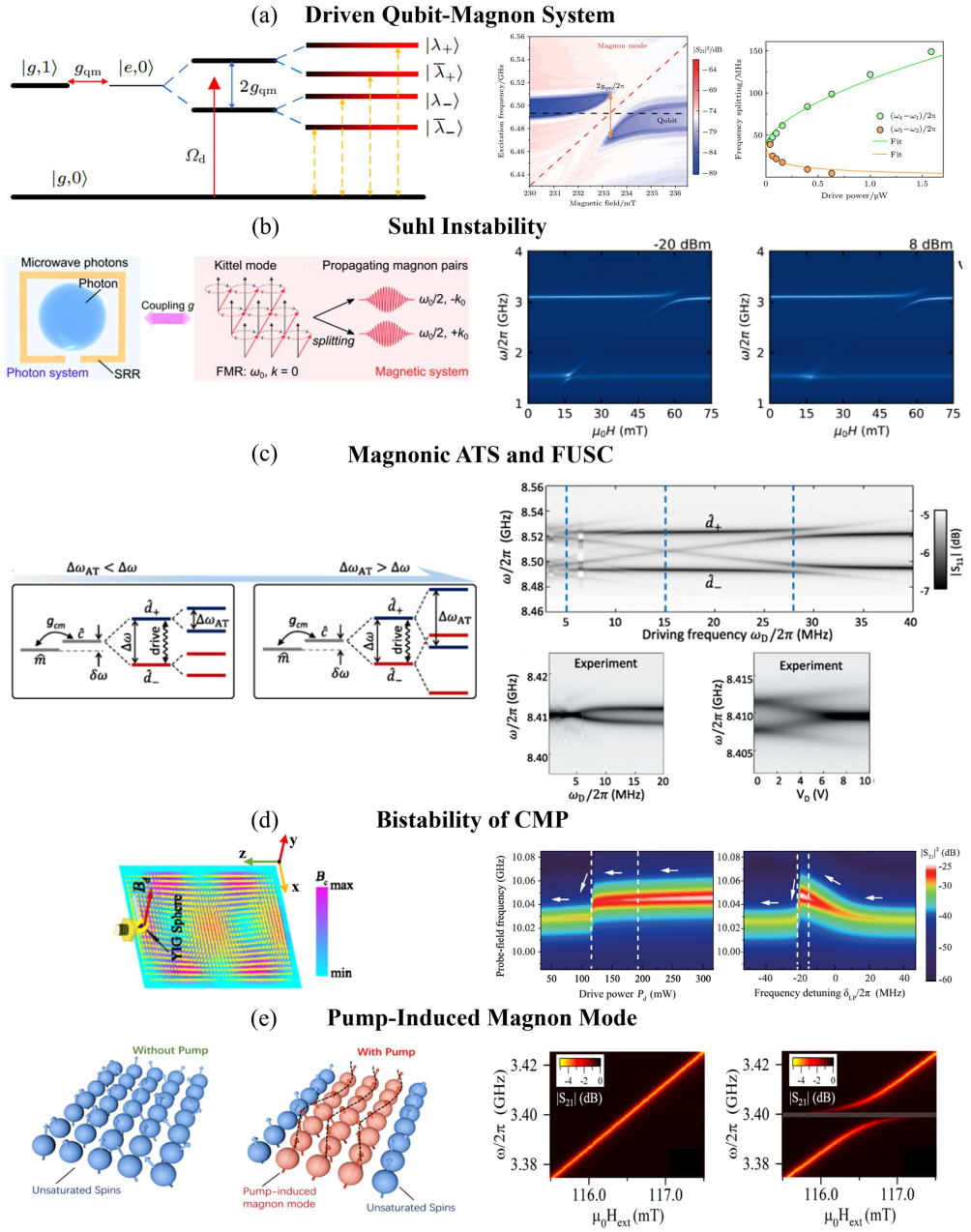


Fig. 2. Mechanisms for constructing continuous magnon states via pumping. (a) Qubit–magnon hybridization leads to pump-dressed states. (b) Suhl instability triggers nonlinear damping via three-magnon scattering. (c) Floquet driving induces tunable hybrid mode splitting. (d) Self-Kerr effect causes frequency shifts and bistability. (e) Pump-induced magnon modes (PIMs) emerge from the cooperative precession of unsaturated spins under pumping. Reproduced with permission from Refs. [22,28,52,57,71].

3.4. Pump-controlled hysteresis of cavity photon–magnon systems via Kerr nonlinearity

When a cavity magnon–photon coupled system is driven by a strong microwave pump, the magnon mode's oscillation deviates from the harmonic approximation and behaves as a Duffing oscillator. Consequently, the CMPs exhibit bistable oscillations. This behavior can be described by an effective Hamiltonian

$$\hat{H}/\hbar = \omega_c \hat{c}^\dagger \hat{c} + \omega_m \hat{b}^\dagger \hat{b} + K \hat{b}^\dagger \hat{b} \hat{b}^\dagger \hat{b} + J(\hat{c}^\dagger \hat{b} + \hat{c} \hat{b}^\dagger) + \Omega_d (\hat{b}^\dagger e^{-i\omega_d t} + \hat{b} e^{i\omega_d t}), \quad (7)$$

where ω_c and ω_m are the frequencies of the cavity photon and magnon modes, respectively; $\hat{c}$, $\hat{b}$ are their annihilation operators; K is the Kerr coefficient stemming from magnetocrystalline anisotropy; J is the coherent coupling strength; and Ω_d, ω_d represent the strength and frequency of the pump field.

This Hamiltonian incorporates the Kerr nonlinearity of the magnon mode[52,76] and leads to a bistable transmission response under continuous-wave pumping. As shown in Fig. 2(d), adjusting the pump power or detuning produces a clear hysteresis loop, with its area continuously tunable *in situ* via pump parameters. This marks the first experimental realization of bistability in CMPs, enabling dynamic control for nonlinear magnonic switching and memory functionalities.

3.5. Pump-tunable coupling between the PIM and WM via phenomenological interaction model

At low magnetic fields, a novel spin-wave excitation, referred to as the pump-induced magnon mode (PIM), emerges in a ferromagnetic insulator sphere. It is phenomenologically understood as the collective precession of unsaturated spins coherently driven by a microwave pump, as illustrated in Fig. 3(a). Unlike conventional magnon modes, the PIM is not tied to intrinsic geometric boundary conditions but is dynamically formed and tunable via the external microwave pump. The PIM enables the realization of strong coupling at low pump power, offering an energy-efficient pathway to engineer coherent magnonic hybrid states.

3.5.1. Theory of PIM–WM coupling

Walker modes (WMs) are quantized magnetostatic spin-wave resonances in a ferromagnetic sphere, under spherical boundary conditions. They appear as standing spin-wave patterns in YIG spheres,[77] interacting with the PIM through magnetic dipole–dipole coupling between their collective spin precessions. When the pump power exceeds the probe power, both modes oscillate at the pump frequency. This allows us to model their interaction using a coupled-mode Hamiltonian

$$\hat{H}/\hbar = \tilde{\omega}_m \hat{a}^\dagger \hat{a} + \tilde{\omega}_d \hat{b}^\dagger \hat{b} + g(\hat{a}^\dagger \hat{b} + \hat{a} \hat{b}^\dagger) + \left(\Omega_d \hat{a}^\dagger e^{-i\omega_d t} + \Omega_d' \hat{b}^\dagger e^{-i\omega_d t} + \text{H.C.}\right). \quad (8)$$

In this equation, the complex mode frequencies $\tilde{\omega}_m = \omega_m - i(\alpha + \gamma)$ and $\tilde{\omega}_d = \omega_d - i\xi$ are defined, where ω_m is the WM frequency and ω_d is the pump frequency. The parameters γ and α represent the external and intrinsic damping rates of the WM, respectively, while ξ is the total damping of the PIM. g is the coupling strength between the PIM and the WM. Ω_d and Ω_d' correspond to the effective intensities of the pump field felt by the WM and PIM, respectively.

By applying the Heisenberg equation of motion to the system Hamiltonian and incorporating the input–output relation, the transmission spectrum of the system can be derived as follows:

$$S_{21} \approx 1 + \frac{\gamma}{i(\omega - \omega_m) - (\gamma + \alpha) + \frac{g^2}{i(\omega - \omega_d) - \xi}}. \quad (9)$$

By further analyzing the dynamical equations, the effective coupling strength can be derived as

$$g = \sqrt{g_0^2 \gamma A_d^2 - (\xi - q A_d)^2 \Delta^2 - (\xi - q A_d)(\gamma + \alpha)}, \quad (10)$$

where g_0 and q are two constants, A_d is the drive amplitude, and Δ is the detuning between the two modes.

The transmission spectrum formula exhibits clear level repulsion behavior, manifesting as an avoided crossing when the pump frequency approaches the WM frequency ω_m. This spectral feature predicts the coherent coupling between the WM and the PIM. Equation (10) indicates that the PIM–WM coupling strength can be tuned by both pump power and frequency, in contrast to the coupling between cavity photons and magnons that remains unaffected by variations in microwave power.

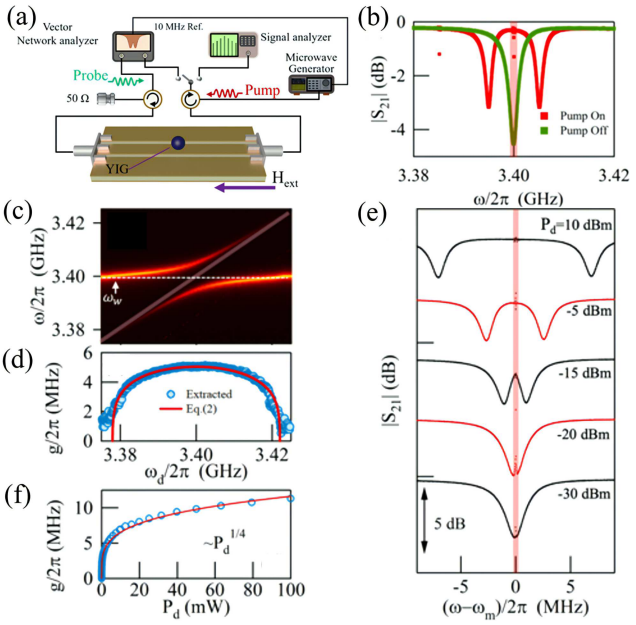


Fig. 3. (a) Schematic diagram of the experimental setup, in which a YIG sphere is placed on a CPW. The probe and pump detect and excite magnon modes in the YIG sphere. (b) The measured transmission magnitudes ($|S_{21}|$) of the Walker mode (2,2,0) upon turning the pump off and on. (c) Transmission spectra of coupled PIM and WM at different pump frequencies. (d) Coupling strength g is extracted from (c), with the red line indicating theoretical calculation. (e) Pump-induced splitting under different pump powers. (f) Coupling strength g is a function of the pump power. Reproduced with permission from Ref. [57].

3.5.2. Experimental features of PIM–WM coupling

To verify the PIM–WM coupling, an experiment is designed in an open electromagnetic environment using a coplanar waveguide (CPW), as illustrated in Fig. 3(a). The key

point lies in the absence of discrete cavity photon modes in the CPW, where magnon–photon avoided crossings are not expected to occur. When the pump field is introduced, mode splitting emerges around the WM frequency (Fig. 3(b)). This contrasts sharply with all previous pump-induced phenomena in hybrid magnonic systems. When we continuously scan the pump frequency while keeping the magnetic field fixed, the linear dispersion of the WM splits into two hybridized resonant modes, producing an anticrossing (Fig. 3(c)). The coupling strength g exhibits an "arch-shaped" dependence on the pump frequency (Fig. 3(d)), unveiling a novel degree of freedom for *in-situ* tunability.

Furthermore, the coupling strength can be tuned by varying the pump power $P_{\rm d}$ according to the relation $g \propto P_{\rm d}^{1/4}$ (Fig. 3(f)). This significantly differs from conventional cavity magnon–polariton systems, where the coupling strength is independent of drive power. This relation is well captured by Eq. (9). Notably, careful analysis of the transmission spectra under different pump powers reveals that mode splitting is already present at a low power of -20 dBm, indicating a low activation threshold for PIM generation (Fig. 3(e)). This enables the construction of strong coupling magnonic systems under low-power conditions.

3.5.3. Hybridization of the PIM and CMP

To extend the controllability of CMPs, the PIM mode is introduced into the cavity system. Due to its dynamic nature, the PIM can be continuously tuned via microwave pumping and strongly couples to normal magnon modes in YIG, enabling hybridization of the CMP and PIM (see Fig. 4(a)).[49] In the experiment, both the pump and probe signals are injected into a CPW-based microwave cavity, forming a three-mode system involving the cavity photon, the WM, and the PIM. The system is described by the following Hamiltonian:

$$\begin{aligned}\hat{H}/\hbar =\ & \tilde{\omega}_{\rm m}\hat{a}^{\dagger}\hat{a}+\tilde{\omega}_{\rm d}\hat{b}^{\dagger}\hat{b}+\tilde{\omega}_{\rm c}\hat{c}^{\dagger}\hat{c} \\ & +g(\hat{a}^{\dagger}\hat{b}+\hat{a}\hat{b}^{\dagger})+J\left(\hat{c}^{\dagger}\hat{b}+\hat{b}^{\dagger}\hat{c}\right) \\ & +\left[{\rm i}\sqrt{\kappa}A_{\rm d}\,{\rm e}^{-{\rm i}\omega_{\rm d}t}\hat{c}^{\dagger}+{\rm H.C.}\right]. \end{aligned} \tag{11}$$

When the pump frequency matches the cavity mode frequency, coherent coupling between the PIM and CMP leads to clear anticrossing in the transmission spectrum, as observed in Fig. 4(b). This confirms the formation of a hybrid PIM–CMP system. Moreover, Fig. 4(c) reveals that the coupling strength g can be continuously tuned by both pump power and frequency — g follows a $P_{\rm d}^{1/4}$ dependence and peaks when the pump frequency approaches the cavity resonance. These two independent parameters provide a route for high-dimensional control of hybrid cavity magnonic systems.

3.5.4. The advantages of the PIM

Based on the above discussion, we identify the following advantages of the PIM.

(1) Breaking boundary condition constraints Unlike conventional magnon modes,[77] which strongly depend on the sample's boundary conditions, PIMs emerge from equilibrium pump-driven excitations. This allows them to exist beyond traditional eigenmode constraints.

(2) Achieving a narrower linewidth PIMs exhibit a linewidth as narrow as 0.55 MHz,[57] lower than that of Walker modes. This implies that the PIM has a lower dissipation rate.

(3) Enabling power-tunable coupling Unlike cavity magnon–photon coupling, the PIM coupling strength can be tuned by adjusting the microwave pump power.

(4) Facilitating nonlinearity at low power PIMs offer distinct advantages for meeting the nonlinear requirements of magnonic systems. Their lower magnetic moment and damping rate enable large-angle precession under low pump powers, making them ideal for tunable, low-power MFC generation.

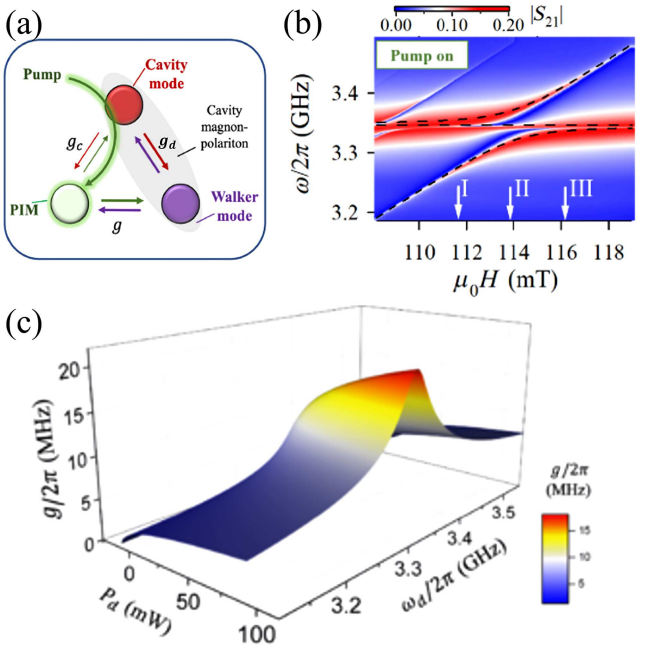


Fig. 4. (a) Schematic diagram of PIM–CMP hybridization. (b) Transmission spectra measured under different magnetic fields when the pump is turned on and the power is set to 10 dBm. The black dashed lines represent the theoretically calculated eigenfrequencies. (c) Coupling strength as a function of pump power and frequency. This figure is adapted from Ref. [49].

4. MFCs and their nonlinearity

Among various magnon-coupled systems, pump-induced nonlinear effects have emerged as a rapidly advancing frontier in both theoretical and experimental studies. A prominent example is the generation of MFCs, which illustrates how dynamic pump control can effectively modulate magnon interactions in the nonlinear regime. MFCs constitute a distinct class of frequency conversion phenomena arising from nonlinear magnon dynamics. These combs hold significant promise for diverse applications, from frequency conversion[52] to high-precision sensing,[68] and may enable ultrafast signal processing in the terahertz (THz) regime.[78] Here, we systematically examine the underlying mechanisms responsible for

MFC generation and analyze the key factors governing their tunability, nonreciprocity, bandwidth expansion, and temporal evolution.

4.1. Magnon–topological magnetic defects

MFCs can arise from nonlinear interactions between propagating spin waves and localized topological magnetic textures, such as skyrmions,[79] bimerons,[80] domain walls (DWs),[81] and magnetic vortices,[82] as illustrated in Fig. 5. Among these, skyrmions have attracted particular attention due to their rich internal dynamics and huge potential for use in information storage. The timeline of MFCs generated by the nonlinear interactions between magnons and skyrmions is summarized in Fig. 6. Peng Yan *et al.*[83] first proposed the generation of MFCs via a nonlinear three-magnon process involving the breathing mode of skyrmions. A strong microwave-driven MFC appears when the microwave field amplitude exceeds a threshold, with comb spacing determined by the frequency of the skyrmion breathing mode. Applying external strain to the magnetic material can tune the generation of MFCs.[84]

Given the strong exchange interaction in antiferromagnetic materials, MFCs in these systems naturally extend into the terahertz domain.[85] Electromagnetic pumping in such systems typically requires higher threshold amplitudes and exhibits distinct frequency-dependent coupling behavior compared to that of their ferromagnetic counterparts.[78] In synthetic ferrimagnets, the comb spacing becomes tunable by adjusting material composition and temperature.[86] Moreover, directional and asymmetric MFC generation can be realized through two-tone microwave excitation. In this case, nonlinear mixing within skyrmion walls and whispering-gallery modes enables unidirectional comb emission. Such effects are observed in waveguide–skyrmion structures.[87] In skyrmion crystal systems, collective breathing modes excited by a single-frequency microwave field can couple with nodal gyration modes, forming low-lying MFCs through three-wave mixing.[88] Bimerons, the in-plane counterparts of skyrmions, also support MFC generation. In antiferromagnetic bimeron systems, the visibility and spectral profile of MFCs are highly anisotropic, depending on both the driving frequency and the propagation direction of the incident magnons.[80]

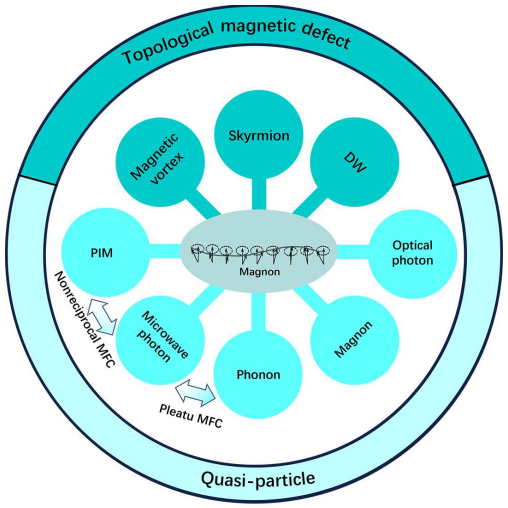


Fig. 5. Coupled magnonic systems involved in MFC generation. In the inner ring, magnons interact with various quasi-particle systems, including phonons, optical photons, microwave photons, and other magnons, as well as with PIMs. These interactions correspond to distinct coupling pathways for realizing MFCs, such as nonreciprocal and plateau MFCs. In the outer ring, magnons couple with topological magnetic textures, including DWs, skyrmions, and magnetic vortices, providing alternative platforms for MFC generation.

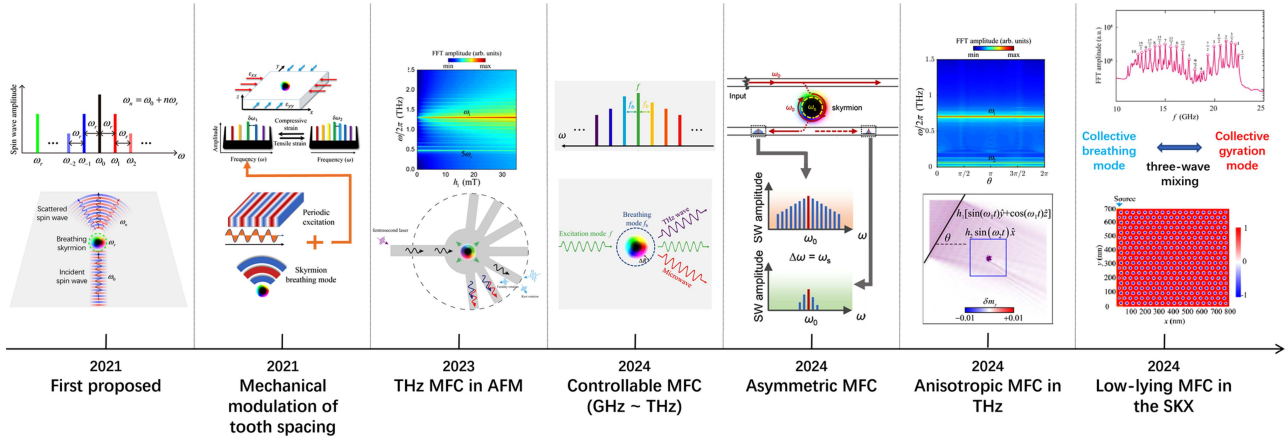


Fig. 6. Timeline of MFCs generated via nonlinear interactions between magnons and skyrmions. Reproduced with permission from Refs. [78,80,83,84,86–88].

4.2. Magnon–quasiparticles

Besides the aforementioned topological magnetic defects, MFCs can also be produced via nonlinear interactions between magnons and other quasiparticles (see Fig. 5), such as phonons, optical photons, microwave photons, and other magnons. The corresponding nonlinear mechanisms include magnetostrictive effects,[68,89,90] Kerr nonlinearity,[91] Brillouin scattering,[92] and four-magnon scattering.[55] Notably, spin-wave frequency combs generated via nonlinear four-magnon interactions in microstructured waveguides marked the first experimental realization of MFCs.[55] Researchers

have proposed the concept of nonreciprocal MFCs in cavity magnonic systems by leveraging photon–magnon coupling, specifically exploiting an asymmetrical nonlinear response in two different directions.[91]

4.2.1. Nonlinear magnetostrictive effect between magnons and phonons

As another class of quasiparticles, phonons can couple with magnons to generate MFCs, as shown in Fig. 5. Microwave pumping modulates the nonlinear interaction between magnons and phonons in magnomechanical systems, leading to the formation of MFCs. The progress of these MFCs arising from the nonlinear magnetostrictive effect between magnons and phonons is summarized in Fig. 7. A single-tone drive can induce magnetostrictive four-wave mixing under high-power conditions.[89] Subsequent experiments[68] revealed that strong pumping leads to heating, which shifts both the magnon and phonon resonant frequencies. Stabilization techniques, such as injection locking, have been used to maintain comb coherence under these conditions. By contrast, a two-tone drive scheme[90] reduces the threshold by generating beat-frequency modulation that enhances magnon–phonon coupling. Further development[93] introduced dissipative coupling in open cavities, enabling ultra broadband MFCs with hundreds of comb lines. These results demonstrate that pump parameters — frequency, amplitude, and spectral composition — directly affect the comb bandwidth, spacing, and stability by shaping the nonlinear response of the hybrid system. MFCs in magnomechanics are evolving toward low-power operation and multimode hybrid control.

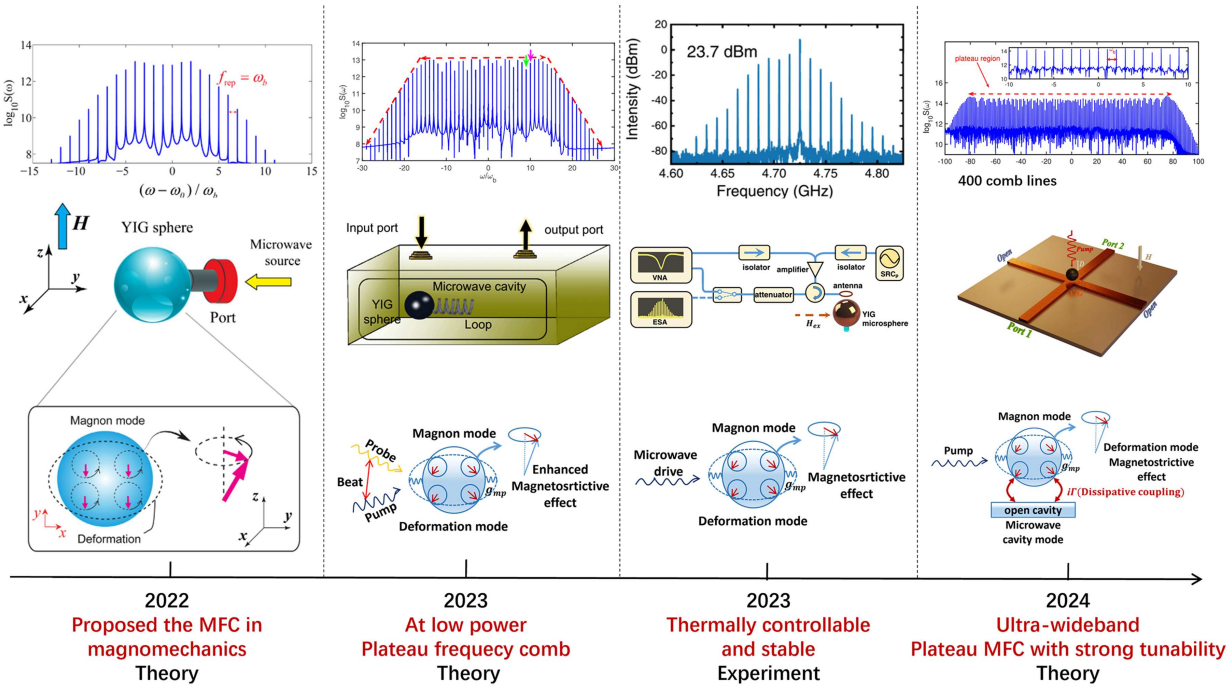


Fig. 7. Progress of MFCs based on nonlinear magnetostriction, from theoretical proposals to low-power, ultra-wideband, and tunable implementations. Reproduced with permission from Refs. [68,89,90,93].

4.2.2. Nonlinear coupling between the PIM and the WM

Among various quasiparticle excitations, the PIM also exemplifies a nonlinear route to the generation of MFCs, as illustrated in Fig. 5.

Conventional MFC generation relies on intrinsic material nonlinearity, which is often weak and requires high power densities or cavity enhancement to exceed the nonlinear threshold.[70]

A promising alternative approach to generating frequency combs exploits the nonlinear dynamics of the PIM–WM hybrid system. This nonlinearity originates from the periodic modulation of the coupling strength between the two modes. This modulation is driven by probe-induced perturbations to the pump field. The PIM–WM hybrid system can be described by a non-Hermitian Hamiltonian. Exceptional points (EPs), defined as the coalescence of both eigenvalues and eigenvectors in non-Hermitian systems,[94,95] inherently exhibit strong sensitivity to perturbations.[70] When the system is tuned to an EP via polarization control of the pump, these perturbations are greatly amplified. As a result, the nonlinear response is significantly enhanced, enabling efficient MFC generation at low power.

Besides enhancing nonlinearity at low power, the combination of EPs and PIMs enables an open, cavity-free architecture suitable for on-chip integration, while inherently avoiding charge noise and Joule heating. More importantly, it allows direct *in situ* tuning of the coupling strength via pump parameters, without relying on material nonlinearity or structural reconfiguration, thereby supporting efficient engineering

of frequency combs.

Based on the original PIM system, we introduce the driving term induced by the weak probe field to account for the oscillations in coupling strength. The Hamiltonian of this coupled PIM–WM system is given by

$$\begin{aligned}\hat{H}/\hbar =\ & \tilde{\omega}_{\rm m}\hat{a}^{\dagger}\hat{a}+\tilde{\omega}_{\rm d}\hat{b}^{\dagger}\hat{b}+g(\hat{a}^{\dagger}\hat{b}+\hat{a}\hat{b}^{\dagger})\\ &+\left(\Omega_{\rm b}\hat{a}^{\dagger}\,{\rm e}^{-{\rm i}\omega_{\rm b}t}+\Omega_{\rm b}'\hat{b}^{\dagger}\,{\rm e}^{-{\rm i}\omega_{\rm b}t}+{\rm H.C.}\right)\\ &+\left(\Omega_{\rm d}\hat{a}^{\dagger}\,{\rm e}^{-{\rm i}\omega_{\rm d}t}+\Omega_{\rm d}'\hat{b}^{\dagger}\,{\rm e}^{-{\rm i}\omega_{\rm d}t}+{\rm H.C.}\right). \quad (12)\end{aligned}$$

In this system, EPs occur at the critical condition $g=\delta_{-}/2$, with $\delta_{-}=\alpha+\gamma-\xi$ representing the damping difference between the PIM and WM modes. At EPs, the two eigenfrequencies coalesce:

$$\tilde{\Delta}_{\pm}=-{\rm i}\frac{\delta_{+}}{2}\pm\sqrt{\left(\frac{\Delta_H}{2}-{\rm i}\frac{\delta_{-}}{2}\right)^2+g^2}, \quad (13)$$

where $\delta_{+}=\alpha+\gamma+\xi$. The presence of EPs enhances the system's sensitivity to perturbations, leading to an increase in nonlinear coupling. Under a two-tone drive, as illustrated in Fig. 8(b), the PIM–KM coupling becomes time-dependent, causing a periodic modulation of the coupling strength

$$g(t)=g_0\sqrt{|B|^2+|\delta b|^2+2|B||\delta b|\cos(\phi_B-\phi_b')}, \quad (14)$$

where B represents the steady-state oscillation amplitude of the PIM, and δb is the fluctuation induced by the probe. The oscillatory nature of $g(t)$ leads to frequency conversion and results in MFC generation.

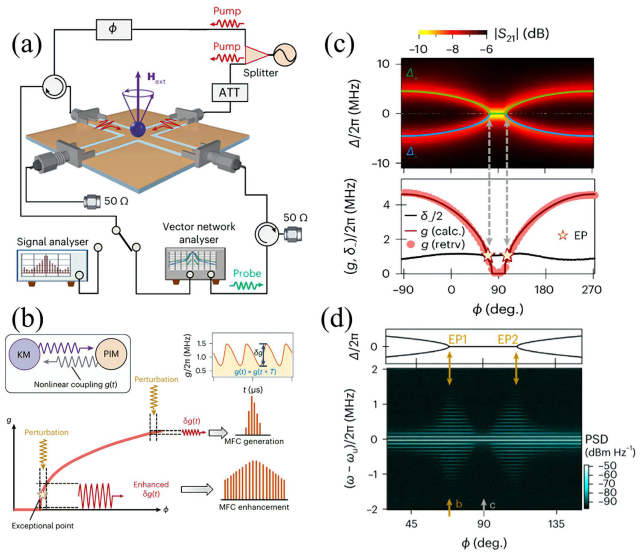


Fig. 8. (a) Schematic diagram of the experimental setup used to generate MFCs by driving a magnetic sphere. (b) Schematic diagram showing the use of EPs to enhance MFCs. The fluctuations of the PIM caused by the slight perturbation of the weak probe modify the conventional constant coupling strength g into periodic oscillations, resulting in nonlinear PIM–KM coupling. (c) Top: transmission spectra measured at different pump polarizations with the magnetic field detuning set to zero. Bottom: extracted g values from the above figure; the black solid line represents the half damping difference. (d) Top: evolution of the two eigenfrequencies with pump polarization. Bottom: radiation spectra under different pump polarizations; the MFC is significantly enhanced near EPs. Reproduced with permission from Ref. [70].

The EP-assisted amplification method has been experimentally verified. A cross-CPW was constructed to adjust the polarization of the pump field at the center of the cross by changing the phase difference (ϕ) between the two orthogonal arms using a phase shifter [Fig. 8(a)].[70] Figure 8(b) reveals the generation mechanism of MFCs and their enhancement near EPs. In the absence of probe perturbation, the PIM–WM coupling strength g is constant (red solid line), depending solely on the pump polarization. The probe introduces a periodic perturbation $\delta g(t)$, causing g to oscillate over time and form a nonlinear coupling. As the system approaches the EPs, the slope of g significantly increases, amplifying the perturbation and resulting in an increase in comb teeth.

Following Eq. (14), we can approach the EP by modulating g via tuning the phase difference between two input microwave pumps (ϕ). Figure 8(c) shows the measured transmission spectra at different ϕ. As the pump field is tuned from right to left circular polarization by adjusting ϕ, the two resonance dips gradually coalesce. The EPs of the coupled system are denoted by stars. Figure 8(d) shows the radiation spectra measured at different polarizations. During the measurement, the frequency of the WM is fixed at the pump frequency, and the probe frequency is set at $\omega_{\rm c}/2\pi=3.0001$ GHz, 0.1 MHz higher than the pump frequency. As the polarization of the pump field is tuned by ϕ, the number of comb teeth near the two EPs dramatically increases from a few to more than 32. This work bridges non-Hermitian physics and MFCs in a cavity-free platform and may find applications in coherent information conversion and sensitive detection.

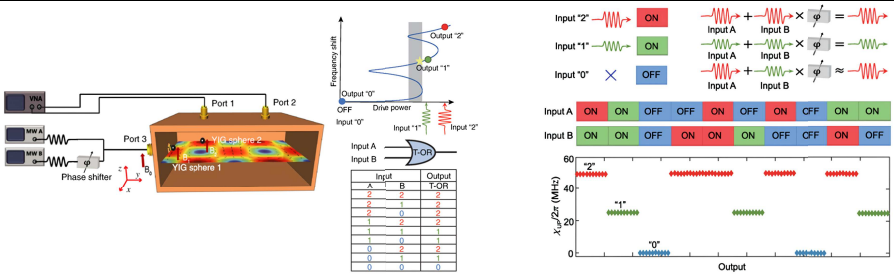
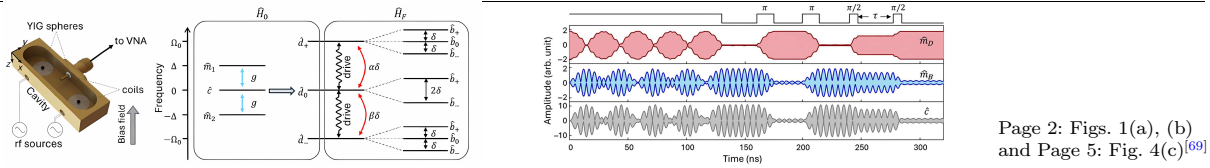
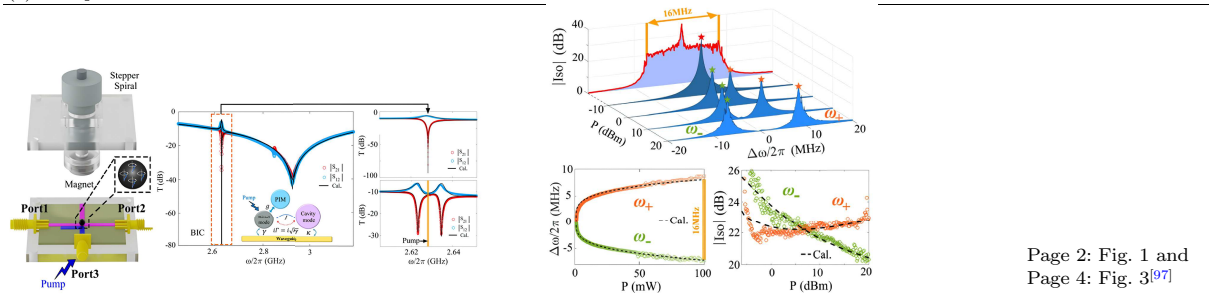
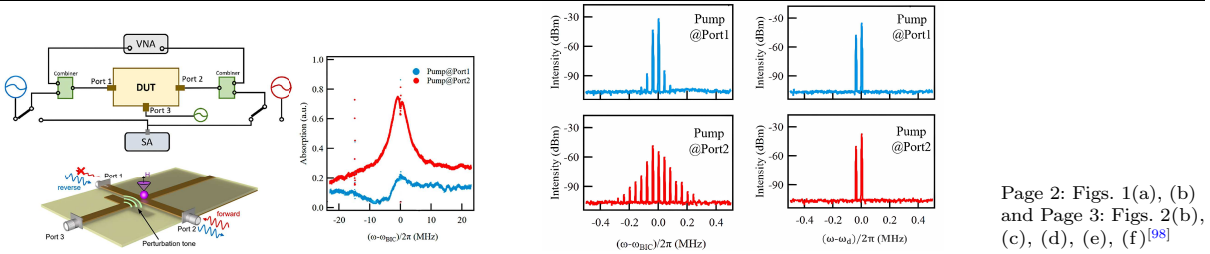
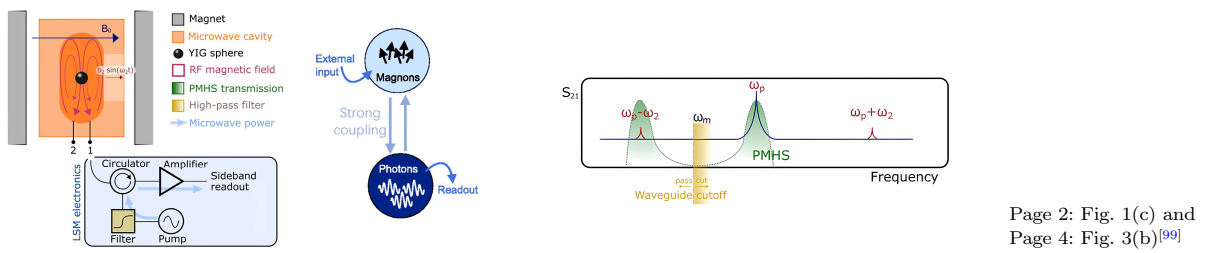
5. Pump-tunable magnonic devices

5.1. Microwave pumping

To date, plenty of cavity magnonic devices have been realized by exploiting the tunability provided by microwave pumping, as summarized in Table 1. In Table 1(a), a ternary logic gate device is realized in a multistable cavity magnonic system.[69] By driving the YIG sphere with variable pump powers, three stable frequency-shifted CMP states emerge from the Kerr nonlinearity, corresponding to logic outputs "0", "1", and "2". The inputs A and B control the total drive power via a phase-engineered combination, and the resulting tristable response enables a compact and power-controllable ternary OR gate. This pump-controlled multistability offers a scalable route toward multivalued logic operations in magnonic computing architectures. In Table 1(b), a cavity magnonic on-demand storage device is demonstrated using Floquet engineering.[96] Two YIG spheres, driven by independently tunable phase-controlled microwave pumps, form collective bright and dark modes.[23] By modulating the amplitude and phase of the pump fields, the central magnon mode

can be dynamically decoupled from or re-coupled to the cavity, effectively achieving reversible isolation and retrieval of the signal. This pump-enabled Floquet control provides a programmable and low-loss approach to magnonic memory, highlighting the role of pump phase and amplitude as dynamic control knobs for hybrid mode formation in cavity magnonics.

Table. 1. Pump-tunable magnonic devices. (a) A tristable cavity system realizes a ternary logic gate. (b) A Floquet-engineered platform stores and retrieves magnon modes on demand. (c) A pump-tunable isolator achieves dynamic nonreciprocity via PIM–BIC hybridization. (d) Nonreciprocal MFC via PIM in a dissipative cavity. (e) Longitudinal spin magnetometer based on phase-modulated CMP and sideband-resolved magnetic field detection. Reproduced with permission from Refs. [69,96–99].

Device and principle	Key features	Reference
(a) Ternary logic gate device		Page 2: Fig. 1 and Page 4: Fig. 4[69]
(b) On-demand storage device		Page 2: Figs. 1(a), (b) and Page 5: Fig. 4(c)[69]
(c) Pump-tunable isolator		Page 2: Fig. 1 and Page 4: Fig. 3[97]
(d) Nonreciprocal MFCs device		Page 2: Figs. 1(a), (b) and Page 3: Figs. 2(b), (c), (d), (e), (f)[98]
(e) Spin-magnetometer		Page 2: Fig. 1(c) and Page 4: Fig. 3(b)[99]

The pump-tunable isolator (see Table (1(c)) demonstrates dynamic electromagnetic control of nonreciprocal microwave transmission through dissipative coupling between a PIM and a bound state in the continuum (BIC).[97] The resonant frequency and spin number of the PIM can be precisely regulated through microwave pump parameters (frequency and power), enabling dynamic reconfiguration of nonreciprocal spectral characteristics without modifying the physical structure of the cavity magnonic system. Experimental results show that direct manipulation of pump parameters achieves con-

trollable nonreciprocal bandwidth (16 MHz) and signal isolation (40 dB), overcoming the inherent limitations of conventional cavity magnonic devices that rely on static magnetic field tuning. This approach enables programmable nonreciprocal mode reconfiguration via microwave pumping control, offering a versatile platform for fast microwave switches, dynamically tunable isolation, and quantum information processing.

Moreover, using this pump-tunable nonreciprocal microwave transmission, a nonreciprocal MFC is realized in a dissipative cavity magnonic device, as shown in Table 1(d).[98] This study experimentally demonstrates nonreciprocal MFC transmission and control in an on-chip dissipative cavity–magnon system by integrating the PIM in a YIG sphere with the asymmetric dissipation of a BIC. Leveraging the strong nonlinearity of PIM under microwave pumping, we achieved unidirectional selectivity with a 14-tooth difference between forward and reverse transmissions through the nonreciprocal absorption at the BICs. This work establishes a paradigm for combining nonlinear magnonics with non-Hermitian cavity–magnon systems, demonstrating potential applications in high-precision frequency metrology, unidirectional signal processing, and multichannel magnon diode design.

In the longitudinal spin magnetometer (LSM) configuration, the pump signal can enhance sensitivity and enable precise detection of oscillating magnetic fields parallel to a static bias field B_0,[99] as illustrated in Table 1(e). By strongly coupling a YIG sphere to a microwave cavity, the CMP is formed, whose resonance frequency becomes highly sensitive to changes in B_0. When a microwave pump is applied at this hybrid resonance ω_p, a weak oscillating magnetic field $b_2 \sin(\omega_2 t)$ modulates the CMP frequency, imparting a phase modulation onto the pump. This phase modulation gives rise to spectral sidebands at $\omega_p \pm \omega_2$, directly encoding the magnetic field information. Through cavity design and frequency engineering, the LSM achieves spectral isolation between the pump signal and the sideband, preventing pump noise from affecting the sideband signal. This enables the use of high pump power to enhance the signal without introducing additional noise. This decoupling of signal and noise channels is a key innovation of the LSM, enabling highly sensitive detection of oscillating magnetic fields.

In summary, by leveraging the tunable dynamics of magnons driven by pumps, a diverse range of device functionalities — computation, isolation, memory, radiation, switching, and sensitive magnetic field detection — has been achieved. These results highlight the potential of pump-controlled coupled magnonic systems as a versatile platform for programmable and nonreciprocal information processing.

5.2. Electric pumping

In practical device-level applications, electrical excitation is currently preferred over direct pumping with photons.

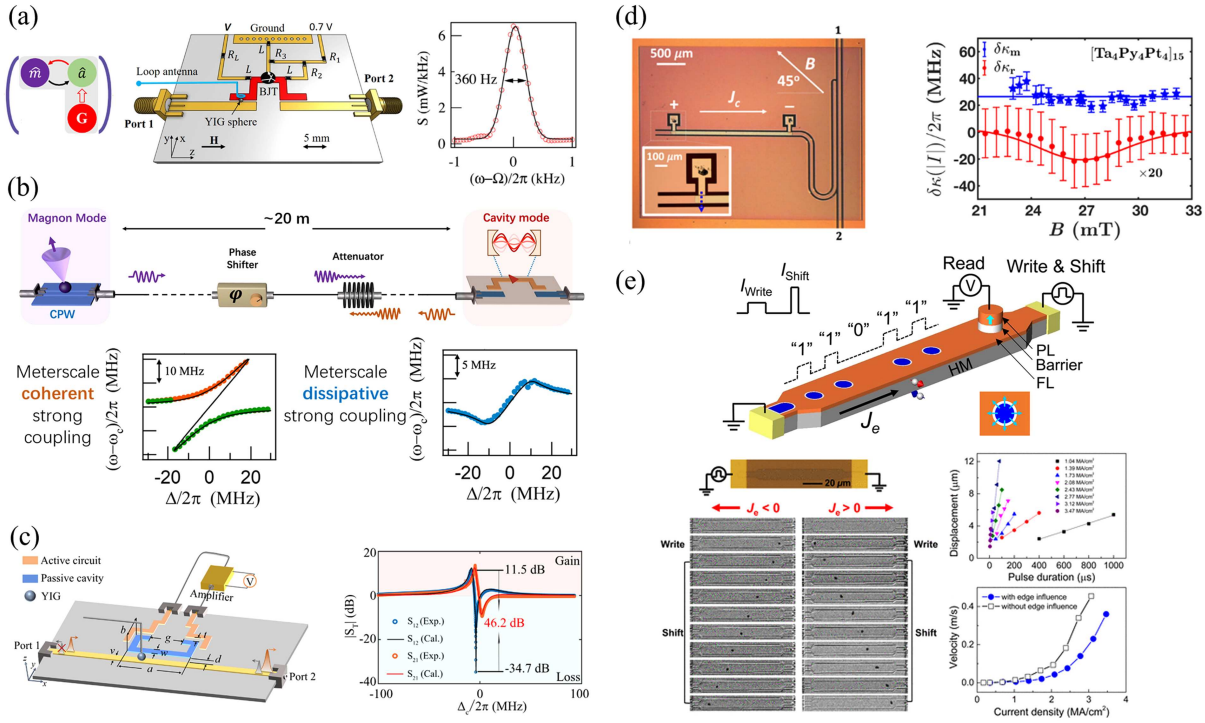


Fig. 9. (a) Left: schematic of the gain-driven polariton. Middle: schematic of the experimental setup for the gain-driven polariton. Right: the power spectral density of the emitted photons measured at $\omega/2\pi = 3.600$ GHz.[100] (b) Top: schematic of the long-range coupling experimental setup. Bottom: bistability of the frequency of the synchronization mode, measured at a transmission coefficient of one, in both coherent and dissipative cases.[101] (c) Left: schematic of the experimental setup for nonreciprocal microwave amplification. Right: measured transmission spectra for the forward and backward directions at $\omega/2\pi = 3.003$ GHz.[102] (d) Left: microscope image of a quarter-wave resonator. Right: the linewidth of magnon and photon modes as functions of the magnetic field, showing current-induced linewidth modulation.[103] (e) Top: schematic of a skyrmion shift memory device. Bottom: experimental process for controlling the movement of individual magnetic skyrmions using current pulses.[104] Reproduced with permission from Refs. [100–104].

This preference is due to the superior controllability of electronic devices, which enables on-demand tuning of system frequency, dissipation, amplitude, and nonlinearity. The high customization capability of modern electronic circuits allows polariton devices to be easily integrated into optoelectronic systems and on-chip architectures, thus facilitating the development of magnon–polariton devices.

In strongly coupled magnonic devices, energy loss is inevitable during operation. By integrating an amplifier into the microwave cavity to form an active cavity–polariton system, energy can be continuously replenished via electrical pumping to compensate for losses in the strongly coupled system (Fig. 9(a)).[100] This manifests itself as narrowed linewidth and enhanced amplitude. This approach offers two main benefits: (1) it achieves phase synchronization and bright mode selection between photons and magnons. Leveraging the gain to maintain polariton coherence realizes coherent microwave amplification based on polaritons (approximately 40 dB) and high-quality coherent microwave emission (with a Q value exceeding 10^9). (2) Further coupling of the active cavity with magnon modes via long coaxial cables, combined with the control of traveling waves using phase shifters, enables strong coupling between magnons and photons over meter-scale distances. The coherent coupling distance is approximately 20 m, while the dissipative coupling distance is about 7.6 m (Fig. 9(b)).[101]

Integrating split resonant rings, amplifiers, and ferromagnetic materials on chip enables nonreciprocal microwave amplification, with 11.5 dB signal amplification in the forward direction and 34.7 dB attenuation in the reverse direction, achieving an isolation ratio of 46.2 dB (Fig. 9(c)).[102] By leveraging the spin Hall effect for electrical control (Fig. 9(d)),[103] dynamic tuning of system dissipation rates and coupling cooperativity is realized. This research holds promise for integrating tunability, on-chip compatibility, and scalability, addressing challenges in practical applications of magnon-based hybrid systems.

A skyrmion shift device operating at room temperature has been realized by manipulating individual skyrmions via current-induced spin–orbit torques (Fig. 9(e)).[104] With low energy dissipation and high data transport efficiency, it offers a scalable approach for future memory storage technologies, potentially bridging the gap between spintronics and conventional data storage solutions.

6. Conclusions

Pump-based control of coupled states in magnonics is a rapidly developing field, with many puzzles waiting to be solved. The coexistence of nonequilibrium dynamics and nonlinear mechanisms in such systems enables rich physical phenomena that transcend conventional paradigms. Traditional electromagnetic/spin-wave boundary confinement conditions lose their dominant role in governing coupled systems when pumping is possible. For example, the introduction of PIM brings new opportunities for the control of magnon Rabi splitting, enabling the coupling to be continuously adjusted through the waveform, amplitude, and frequency of the pump, instead of being confined to discrete modes determined by microwave structures or spin sample sizes. Such increased control flexibility also advances the development of nonlinear effects in magnonics. For example, pumped magnons can better serve the exploration of magnon frequency combs, multistability, or chaotic[105,106] physics.

Thanks to the rapid evolution and powerful capabilities of pumping techniques, electromagnetic wave pumping can introduce time-domain control, along with the closely related Floquet engineering and time-varying materials. These advances may give rise to novel concepts and behaviors not found in existing coupled magnonics systems. Meanwhile, electrical pumping, with its precise matching of gain and loss to the zero-dissipation condition, can induce interesting phenomena such as magnon–photon synchronization, high-coherence radiation, and long-range (meter-scale) strong coupling. Moreover, the study of these physical principles is not limited to the specific realm of magnons as a carrier. Instead, it holds promise for applications in many cutting-edge and interdisciplinary fields of modern physics. Given the excellent ability of magnons to form hybrid states with high coherence, we anticipate that control methods based on pumping coupled magnons can make further contributions to various fields.

The development of quantum information processing brings both opportunities and challenges for pump-controlled magnonics. To realize its merits in practical quantum systems, it is essential to suppress power consumption and thermal effects while enhancing scalability. Regarding power consumption, the generation of PIMs and their strong coupling behaviors requires milliWatt-level (nT level)[48]) microwave power.[57] Concerning thermal effects, the heat generated by the PIM-based isolator is roughly estimated to be less than 1.34 mW, comparable to the heat dissipated by the active devices used in dilution refrigerators.[97] Moreover,with meter-scale strong photon–magnon coupling realized in electrically pumped devices, traveling-wave control can be used to facilitate the construction of large-scale quantum networks.[101] To meet the demands of quantum applications, it is necessary to develop field control techniques with higher sensitivity and to lower the nonlinear threshold of the pumping process in order to reduce energy consumption. Coupling with superconducting circuits may help lower conductive loss and improve thermal management. It is also important to explore strategies for suppressing decoherence under pumped excitation to better support device scalability. Current research has shown positive results for pump-controlled magnons. Further resolving technical challenges will better reveal their advantages for advanced information processing and related quantum control.

Appendix A: Summary of pump-induced coupled magnonic states

Table A1. Summary of pump-induced continuously tunable coupled magnonic states.

Section	Continuously tunable feature	Hybrid systems	Underlying mechanism
3.1	Dual-frequency splitting that evolves with drive power (double dressing)	Qubit–magnon	Parametric microwave driving of the qubit
3.2	Gradual suppression and collapse of avoided crossing	Magnon–cavity photon	Suhl instability via three-magnon scattering
3.3	Drive-dependent mode splitting (ATS), transition to Floquet ultrastrong coupling	Magnon–cavity photon	Floquet modulation with periodic driving of magnon frequency
3.4	Bistable transmission and hysteresis loops controlled by pump power and detuning	Magnon–cavity photon	Kerr nonlinearity induced by magnetocrystalline anisotropy
3.5	Level repulsion and frequency comb enabled at low pump powers	PIM–WM	Phenomenologically understood as the coupling between conventional magnons and pump-induced magnons

Appendix B: List of abbreviations

Table B1. List of abbreviations and their full names used in the manuscript.

Abbreviation	Full name	Definition
CMP	Cavity magnon polaritons	Hybrid quasiparticles formed by magnon–microwave cavity photon coupling.
WM	Walker modes	Spin-wave eigenmodes in a YIG sphere, obtained as analytical solutions of the coupled Maxwell and Landau–Lifshitz equations under spherical boundary conditions.
PIM	Pump-induced magnon mode	A spin-wave excitation induced by a microwave pump, phenomenologically understood as originating from the collective precession of unsaturated spins in a YIG sphere.
EP	Exceptional point	A non-Hermitian spectral degeneracy where two or more eigenvalues coalesce.
ATS	Autler–Townes splitting	A coherent-field-induced splitting of energy levels into doublets, with a splitting magnitude proportional to the drive strength and independent of quantum interference.
FUSC	Floquet ultrastrong coupling	A dynamic coupling regime where Floquet-induced splitting approaches or exceeds the energy level spacing, breaking the rotating-wave approximation and involving counter-rotating interactions.

Acknowledgements

This work has been supported by the Strategic Priority Research Program of the Chinese Academy of Sciences (Grant No. XDB0580000), the National Natural Science Foundation of China (Grant Nos. 12204306, 12122413, 12227901, 12474120, and U23A6002), the Science and Technology Commission of Shanghai Municipality (Grant Nos. 23JC1404100 and 22JC1403300), the National Key R&D Program of China (Grant Nos. 2022YFA1404603 and 2023YFA1406604), the Shandong Provincial Natural Science Foundation, China (Grant No. ZR2024YQ001), and the Qilu Young Scholar Programs of Shandong University.

References

[1] Takeuchi S, Kim J, Yamamoto Y and Hogue H H 1999 *Appl. Phys. Lett.* **74** 1063
[2] Cova S D and Ghioni M 2011 *IEEE Photonics Journal* **3** 274
[3] Kulish M and Malysh M 2022 *Semicond. Phys., Quantum Electron. Optoelectron.* **25** 68
[4] Hao H, Zhao Q Y, Huang Y H, Deng J, Yang F, Ru S Y, Liu Z, Wan C, Liu H, Li Z J, *et al*. 2024 *Light: Science & Applications* **13** 25
[5] Wu W, Chen M, Zhang Z, Liu X and Dong Y 2018 *Science China Information Sciences* **61** 1
[6] Zhou X, Bec J, Yankelevich D and Marcu L 2021 *Opt. Express* **29** 20105
[7] Yotter R A and Wilson D M 2003 *IEEE Sensors Journal* **3** 288
[8] Pisani F, Gacemi D, Vasanelli A, Li L, Davies A G, Linfield E, Sirtori C and Todorov Y 2023 *Nat. Commun.* **14** 3914
[9] Hagenmüller D, Schachenmayer J, Schütz S, Genes C and Pupillo G 2017 *Phys. Rev. Lett.* **119** 223601
[10] Orgiu E, George J, Hutchison J A, Devaux E, Dayen J F, Doudin B, Stellacci F, Genet C, Schachenmayer J, Genes C, *et al*. 2015 *Nat. Mater.* **14** 1123
[11] Hu S Q, Zhao H, Lian C, Liu X B, Guan M X and Meng S 2022 *npj Quantum Materials* **7** 14
[12] Liu X B, Hu S Q, Chen D, Guan M, Chen Q and Meng S 2022 *Nano Lett.* **22** 4800
[13] Zhao W M, Zhu L, Nie Z, Li Q Y, Wang Q W, Dou L G, Hu J G, Xian L, Meng S and Li S C 2022 *Nat. Mater.* **21** 284
[14] Sun Z, Murakami Y, Xuan F, Kaneko T, Golež D and Millis A J 2024 *Phys. Rev. Lett.* **133** 217002
[15] Chen Y J, Cain J D, Stanev T K, Dravid V P and Stern N P 2017 *Nat. Photonics* **11** 431
[16] Galiffi E, *et al*. 2024 *Nature Reviews Materials* **9** 9
[17] Ginzburg P 2016 *Reviews in Physics* **1** 120
[18] Gilleo M and Geller S 1958 *Phys. Rev.* **110** 73
[19] Cao Y, Yan P, Huebl H, Goennenwein S T and Bauer G E 2015 *Phys. Rev. B* **91** 094423
[20] Yao B, *et al*. 2019 *Commun. Phys.* **2** 161
[21] Liu C, *et al*. 2018 *Nat. Commun.* **9** 738
[22] Xu J, Zhong C, Han X, Jin D, Jiang L and Zhang X 2020 *Phys. Rev. Lett.* **125** 237201
[23] Zhang X, Zou C L, Zhu N, Marquardt F, Jiang L and Tang H X 2015 *Nat. Commun.* **6** 8914
[24] Zhu H, Shi H, Tang Z and Tang B 2024 *Chin. Phys. B* **33** 037503
[25] Huebl H, *et al*. 2013 *Phys. Rev. Lett.* **111** 127003
[26] Zeng Z and Yan P 2025 *Phys. Rev. Lett.* **134** 026701
[27] Cornelissen L, Liu J, Duine R, Youssef J B and Van Wees B 2015 *Nat. Phys.* **11** 1022
[28] Tabuchi Y, *et al*. 2015 *Science* **349** 405

[29] Xu D, Wang Y P, Li T F and You J Q 2022 *Acta Phys. Sin.* **71** 150302 (in Chinese)
[30] Zhu L T, Zhu X Y, Yue Z C, Tu T and Li C F 2025 *Chin. Phys. B* **34** 030302
[31] Berk C, *et al*. 2019 *Nat. Commun.* **10** 2652
[32] Liu S, *et al*. 2021 *Phys. Rev. Lett.* **127** 097401
[33] Zhang X, *et al*. 2014 *Phys. Rev. Lett.* **113** 156401
[34] Li Y, *et al*. 2019 *Phys. Rev. Lett.* **123** 107701
[35] Wang X, Qiu Q Y, Huang K W and Xiong H 2023 *Phys. Rev. A* **108** 063715
[36] Wang N, Li S Y, Yu L and Zhu A D 2024 *Phys. Rev. B* **110** 144424
[37] Yu W, Yu T and Bauer G E 2020 *Phys. Rev. B* **102** 064416
[38] Lachance-Quirion D, *et al*. 2019 *Applied Physics Express* **12** 070101
[39] Soykal Ö O and Flatté M 2010 *Phys. Rev. Lett.* **104** 077202
[40] Grigoryan V L and Xia K 2019 *Phys. Rev. B* **100** 014415
[41] Yu W, Wang J, Yuan H and Xiao J 2019 *Phys. Rev. Lett.* **123** 227201
[42] Rao J W, *et al*. 2020 *Phys. Rev. B* **101** 064404
[43] Harder M, Yao B, Gui Y and Hu C M 2021 *J. Appl. Phys.* **129** 201101
[44] Wang Y P, Rao J W, Yang Y, Xu P C, Gui Y S, Yao B M, You J Q and Hu C M 2019 *Phys. Rev. Lett.* **123** 127202
[45] Yu T, *et al*. 2020 *Phys. Rev. Lett.* **124** 107202
[46] Yu W, Yu T and Bauer G E 2020 *Phys. Rev. B* **102** 064416
[47] Zhang X, Bauer G E and Yu T 2020 *Phys. Rev. Lett.* **125** 077203
[48] Rao J, Wang Y P, Chen Z, Yao B, Zhao K and Wei C, Wang C, Li R, Bai L and Lu W 2025 *Phys. Rev. Lett.* **135** 066704
[49] Zhang C, Rao J, Wang C, Chen Z, Zhao K, Yao B, Xu X G and Lu W 2023 *Phys. Rev. A* **20** 024074
[50] Chumak A, Melkov G, Demidov V, Dzyapko O, Safonov V and Demokritov S 2009 *Phys. Rev. Lett.* **102** 187205
[51] Alekseev S, Dizhur S, Polzikova N, Luzanov V, Raevskiy A, Orlov A, Kotov V and Nikitov S 2020 *Appl. Phys. Lett.* **117** 072408
[52] Wang Y P, *et al*. 2018 *Phys. Rev. Lett.* **120** 057202
[53] Zhang X, Zhu N, Zou C L and Tang H X 2016 *Phys. Rev. Lett.* **117** 123605
[54] Nowik-Boltyk P, Borisenko I, Demidov V and Demokritov S 2019 *Ukrainian Journal of Physics* **64** 938
[55] Hula T, *et al*. 2022 *Appl. Phys. Lett.* **121** 112404
[56] Zhang X, *et al.* 2016 *Science Advances* **2** e1501286
[57] Rao J, Yao B, Wang C, Zhang C, Yu T and Lu W 2023 *Phys. Rev. Lett.* **130** 046705
[58] Lyons T P, *et al*. 2023 *Phys. Rev. Lett.* **131** 196701
[59] Kurkin M, *et al*. 2008 *Phys. Rev. B* **78** 134430
[60] Shi J, *et al*. 2023 *Advanced Science* **10** 2205903
[61] Harder M and Hu C M 2018 *Solid State Phys.* **69** 47
[62] Jäckl M, *et al*. 2017 *Phys. Rev. X* **7** 021009
[63] Zhou L, *et al*. 2024 *Nat. Commun.* **15** 7782
[64] Boventer I, *et al*. 2020 *Phys. Rev. Research* **2** 013154
[65] Boventer I, *et al*. 2019 *New J. Phys.* **21** 125001
[66] Demokritov S O, *et al*. 2006 *Nature* **443** 430
[67] Borisenko I, *et al*. 2020 *Nat. Commun.* **11** 1691
[68] Xu G T, *et al*. 2023 *Phys. Rev. Lett.* **131** 243601
[69] Shen R C, *et al*. 2021 *Phys. Rev. Lett.* **127** 183202
[70] Wang C, *et al*. 2024 *Nat. Phys.* **20** 1139
[71] Lee O, *et al*. 2023 *Phys. Rev. Lett.* **130** 046703
[72] Zhang Y H 2024 *Critical Coupling and Floquet in Cavity Magnonics* Master's thesis University of Manitoba Winnipeg, Manitoba, Canada
[73] Oka T and Kitamura S 2019 *Annual Review of Condensed Matter Physics* **10** 387
[74] Autler S H and Townes C H 1955 *Phys. Rev.* **100** 703
[75] Anisimov P M, Dowling J P and Sanders B C 2011 *Phys. Rev. Lett.* **107** 163604
[76] Wang Y P, *et al*. 2016 *Phys. Rev. B* **94** 224410
[77] Walker L R 1957 *Phys. Rev.* **105** 390
[78] Yao X, *et al*. 2023 *Phys. Rev. B* **108** 134427
[79] Abdulrazak T, Liu X, Jin Z, Cao Y and Yan P 2024 *Chin. Phys. B* **33** 087503
[80] Zhang C, *et al*. 2024 *Appl. Phys. Lett.* **125** 052401
[81] Zhou Z W, *et al*. 2021 *J. Magn. Magn. Mater.* **534** 168046
[82] Heins C, Kákay A, Kim J V, Hlawacek G, Fassbender J, Schultheiss K and Schultheiss H 2025 arXiv preprint arXiv:2501.05080
[83] Wang Z, Yuan H, Cao Y, Li Z X, Duine R A and Yan P 2021 *Phys. Rev. Lett.* **127** 037202
[84] Sun J, Shi S and Wang J 2022 *Advanced Engineering Materials* **24** 2101245
[85] Qiu H, *et al*. 2023 *Advanced Science* **10** 2300512
[86] Liu Y, *et al*. 2024 *Phys. Rev. B* **109** 174412
[87] Liang X, Cao Y, Yan P and Zhou Y 2024 *Nano Lett.* **24** 6730
[88] Liu X, *et al*. 2024 *Phys. Rev. B* **110** 184413
[89] Xiong H 2023 *Fundamental Research* **3** 8
[90] Liu Z X, Peng J and Xiong H 2023 *Phys. Rev. A* **107** 053708
[91] Wang X, Huang K W, Qiu Q Y and Xiong H 2023 *Chaos, Solitons & Fractals* **176** 114137
[92] Liu Z X and Li Y Q 2022 *Photonics Research* **10** 2786
[93] Liu Z X 2024 *Appl. Phys. Lett.* **124** 032403
[94] Dembowski C, *et al*. 2001 *Phys. Rev. Lett.* **86** 787
[95] Miri M A and Alu A 2019 *Science* **363** eaar7709
[96] Pishehvar A, *et al*. 2025 *Phys. Rev. A* **23** 024053
[97] Chen Z, Rao J, Zhao K, Yang F, Wang C, Yao B and Lu W 2024 *Appl. Phys. Lett.* **125** 042403
[98] Zhao K, *et al*. 2025 *AIP Advances* **15** 015015
[99] Crescini N, *et al*. 2020 *Appl. Phys. Lett.* **117** 144001
[100] Yao B, *et al*. 2023 *Phys. Rev. Lett.* **130** 146702
[101] Rao J, *et al*. 2023 *Phys. Rev. Lett.* **131** 106702
[102] Wang Z Y, *et al*. 2023 *Appl. Phys. Lett.* **123** 153904
[103] Hou J T, *et al*. 2024 *Appl. Phys. Lett.* **124** 072401
[104] Yu G, *et al*. 2017 *Nano Lett.* **17** 261
[105] Peng J, Liu Z X, Yu Y F and Xiong H 2024 *Phys. Rev. A* **110** 053704
[106] Wang M, *et al*. 2019 *IEEE Photonics Journal* **11** 1